

Nonlinear Bubble Dynamics And The Effects On Propagation Through Near-Surface Bubble Layers

Timothy G. Leighton

Institute of Sound and Vibration Research, University of Southampton, Highfield, Southampton UK

Abstract. Nonlinear bubble dynamics are often viewed as the unfortunate consequence of having to use high acoustic pressure amplitudes when the void fraction in the near-surface oceanic bubble layer is great enough to cause severe attenuation (e.g. >50 dB/m). This is seen as unfortunate since existing models for acoustic propagation in bubbly liquids are based on linear bubble dynamics. However, the development of nonlinear models does more than just allow quantification of the errors associated with the use of linear models. It also offers the possibility of propagation modeling and acoustic inversions which appropriately incorporate the bubble nonlinearity. Furthermore, it allows exploration and quantification of possible nonlinear effects which may be exploited. As a result, high acoustic pressure amplitudes may be desirable even in low void fractions, because they offer opportunities to gain information about the bubble cloud from the nonlinearities, and options to exploit the nonlinearities to enhance communication and sonar in bubbly waters. This paper presents a method for calculating the nonlinear acoustic cross-sections, scatter, attenuations and sound speeds from bubble clouds which may be inhomogeneous. The method allows prediction of the time dependency of these quantities, both because the cloud may vary and because the incident acoustic pulse may have finite and arbitrary time history. The method can be readily adapted for bubbles in other environments (e.g. clouds of interacting bubbles, sediments, structures, *in vivo*, reverberant conditions etc.). The possible exploitation of bubble acoustics by marine mammals, and for sonar enhancement, is explored.

NONLINEAR THEORY

Acoustic propagation through bubbly water has been modeled only with the introduction of the assumption of bubble linearity, or linearisation of the bubble dynamics, at an early stage. Probably the most notable example is the pioneering work of Commander and Prosperetti [1], which has been cited over 100 times since publication and used in many more acoustic investigations. If this linearisation is not done, not only do the formulations become inherently more complicated, but several useful mathematical techniques are not valid. These include complex representation of oscillations, small amplitude expansions, Green's function, Fourier transforms, superposition and addition of solutions. This paper describes a nonlinear approach.

Consider a cloud of bubbly water (having volume V_c and sound speed c_c and bulk modulus B_c). It is made up of a volume V_w of bubble-free water (having sound speed c_w and bulk modulus B_w) and a volume V_g of free gas (having sound speed c_g and bulk modulus B_g) distributed in a population of bubbles. Hence

$$V_c = V_w + V_g \quad (1)$$

Mass conservation is simply expressed by multiplication of the volumes with the respective densities (of cloud, ρ_c ; bubble free water, ρ_w ; and gas, ρ_g), i.e.

$$\rho_c V_c = \rho_w V_w + \rho_g V_g \quad (2)$$

When an acoustic wave passes through the bubbly liquid, the oscillatory pressures applied to the bubbles cause them to undergo pulsation. Under the assumption that each of the three media separately conserve mass, the differential of (2) with respect to the applied pressure P is, of course, zero. In an infinite body of either water or gas that contains no dissipation (an assumption which will shortly be examined further), sound speeds (c_w and c_g respectively) may be defined:

$$c_\zeta^2 = \frac{B_\zeta}{\rho_\zeta} = \left(\frac{\partial P(\rho, S)}{\partial \rho} \right)_\zeta \quad (\zeta = w, g) \quad (3)$$

where S is the entropy and the subscript ζ refers to application to bubble-free water (w) or gas (g) throughout (3). Similarly, differentiation of (1) with respect to the applied pressure gives, with (3), the relationship between the bulk moduli

$$\frac{1}{B_c} = \frac{V_w}{V_c} \frac{1}{B_w} + \frac{V_g}{V_c} \frac{1}{B_g} \quad (4)$$

Let us define a function ξ_c (which is not an inherent property of the bubble cloud in the thermodynamic sense), equal to the root of the ratio of the bulk modulus of the bubbly water to its density, which with (4) gives:

$$\xi_c = \sqrt{\frac{B_c}{\rho_c}} = \sqrt{\left(\frac{V_c}{\rho_w V_w + \rho_g V_g} \right) / \left(\frac{V_w}{V_c B_w} + \frac{V_g}{V_c B_g} \right)} \approx c_w \left(1 + \frac{B_w V_g(t)}{V_c B_g} \right)^{-1/2} \quad (5)$$

where the final approximate form is valid under low void fraction conditions [2]. If there were no dissipation, the quantity ξ_c could be identified with the sound speed in bubbly water. However such an identity is not rigorous for lossy bubble clouds [2].

Evaluation of (5) requires calculation of the bulk modulus of the gas, as it is distributed through a (presumably) numerous population of bubbles pulsating with a broad range of amplitudes, phases, frequency content, damping and start times. The inhomogeneous bubbly water must be divided into volume elements which are sufficiently small to ensure that all the bubbles in that element are subjected to the same pressure change $dP(t)$ simultaneously (the use of d indicating an intention to use or calculate the quantity numerically). This would allow calculation of a value ξ_c for each volume element, since from (3) the bulk modulus B_{g_l} of the gas within the l^{th} volume element is related to the volume changes dV_i of the I bubbles in that volume element:

$$\frac{1}{B_{g_l}} = -\frac{1}{V_{g_l}} \sum_{i=1}^I \frac{dV_i}{dP_l} \quad (6)$$

where P_l denotes the pressure in the l^{th} element. Consider one such volume element V_{c_l} of a cloud which has total volume $V_c = \sum_{l=1}^L V_{c_l}$. Substituting (6) into (5) gives ξ_{c_l} , the time history of ξ_c within the volume element V_{c_l} :

$$\xi_{c_l} \approx c_w \left(1 - \frac{\rho_w c_w^2}{V_{c_l}} \sum_{i=1}^l \frac{dV_i}{dP_l} \right)^{-1/2} \quad (7)$$

To understand the meaning of this quantity, consider that, if the system were linear, monodisperse and lossless, dV_i/dP_l would be a constant throughout the steady-state oscillatory cycle: In pressure-volume space, as one progressed throughout the oscillatory cycle one would move back and forth along a locus of points mapping out a straight line. The constant gradient of that line could be related to the sound speed in the cloud through (7), which would equal the constant ξ_{c_l} . If the monodisperse system were nonlinear and lossless, dV_i/dP_l would vary through the cycle, and the single line mapped out by the locus of points in pressure-volume space would not be straight. In this case the sound speed would vary through the oscillatory cycle, and could again be identified with ξ_{c_l} through (7). This could then be related to a sound speed for nonlinear propagation. If however dissipation occurs, the locus of points in the pressure-volume plane would, during a single oscillatory cycle, map out a finite area. In such circumstances ξ_{c_l} cannot strictly be identified with any sound speed. If dissipation is very small then one might identify a characteristic value of dV_i/dP_l which is not much different from the true value for most of the acoustic cycle; for the linearised case, this is in effect what Commander and Prosperetti do [1]. This will be discussed further in relation to Figure 4.

To evaluate (7), the bubble population of the volume element is classified into J discrete bins according to bubble size. Every individual bubble in the j^{th} bin is replaced by another bubble which oscillates with radius $R_j(t)$ and volume $V_j(t)$ (about equilibrium values of R_{0_j} and V_{0_j}), such that the total number of bubbles N_j and total volume of gas $N_j V_j(t)$ in the bin remain unchanged by the replacement. If the bin width increment is sufficiently small ($1 \mu\text{m}$ is normally chosen), the time history of every bubble in that bin should closely resemble $V_j(t) = V(R_{0_j}, t)$ (the sensitivity being greatest around resonance). Hence the total volume of gas in the l^{th} volume element of bubbly water is $V_{g_l}(t) = \sum_{j=1}^J N_j(R_{0_j}, t) V_j(t) = V_{c_l} \sum_{j=1}^J n_j(R_{0_j}, t) V_j(t)$, where $n_j(R_{0_j}, t)$ is the number of bubbles per unit volume of bubbly water within the j^{th} bin. Expressing (7) in terms of this bin scheme gives:

$$\xi_{c_l} \approx c_w \left(1 - \rho_w c_w^2 \sum_{j=1}^J n_j(R_{0_j}) \frac{dV_j}{dP_l} \right)^{-1/2} \quad (8)$$

Crucially (8) provides a *generic framework into which any bubbly dynamics model may be inserted* (giving $dV_j(t)/dP_i(t)$ appropriate to bubbles in free field or reverberation, *in vivo*, in structures or sediments, or in clouds of interacting bubbles, etc. as the chosen model dictates). This will be discussed later. First, the following section will use a speculative application to illustrate the general characteristics in the linear monochromatic steady state limit.

REDUCTION OF THEORY TO LINEAR LIMIT

Equation (8) contains low-void fraction limitations identical to those discussed by Commander and Prosperetti [1], to be used in an appropriate propagation model [1-4]. However so far no assumptions of small amplitude, steady state, monochromatic or linear bubble pulsations have been included, nor have the bubbles and their wall motions been assumed to be spherically symmetric. If these assumptions are introduced, the linear formulation of Commander and Prosperetti [1] is readily obtained from (8) [2]. The qualitative effect on the sound speed, predicted by such linear formulations when bubbles are added to previously bubble-free water, is well-known. In quasi-static conditions, the addition to gas bubbles to liquid will reduce its bulk modulus (since in (3) a given positive ∂P will cause a much larger compression $\partial \rho$ because of the reduction in volume of the bubbles). It will also reduce the density, but to a lesser amount, and therefore the net result is a reduction in the sound speed (see (3); alternatively, note that in a binomial expansion of (5), all the terms in $B_w V_g / (V_c B_g)$ are positive under quasi-static conditions). Consider now a monodisperse population of bubbles. As the driving frequency increases towards resonance, the amplitude of oscillation increases, and therefore so will the reduction in sound speed engendered by the presence of these bubbles. However, when the driving frequency exceeds the resonance of the bubbles, they are inertia-controlled: The compressive half-cycle of the driving field dP coincides with a bubble expansion, because of the change in the phase relation between them (which changes the sign of dV_i/dP_i in (7)). Hence at frequencies greater than resonance, the presence of bubbles causes an increase in sound speed. The magnitude of the effect becomes smaller as the frequency increases to values further from the bubble resonance (and the amplitude of pulsation decreases), until at very high frequencies the sound speed is identical to the bubble-free condition.

This linear scheme has been put to valuable use in modeling the propagation of sound through the near-surface bubble layer, where for frequencies sufficiently low to drive the bubbles in stiffness-mode, the zone can be upwardly refracting, generating a waveguide [5-7]. However a more fanciful application might explain the mystery of the mechanism by which humpback whales (*Megaptera novaeangliae*) exploit bubble nets to catch fish [8]. It has been known for decades that up to 30 whales might dive deep and then release bubbles to form the walls of a cylinder, the interior of which is relatively bubble-free (Fig. 1a,b) [9]. The prey are trapped within this cylinder, for reasons previously unknown, before the whales lunge feed on them from below (Fig. 1c). When the whales form such nets, they emit very loud, ‘trumpeting feeding calls’,

the available recordings containing energy up to at least 4 kHz. A suitable void fraction profile would cause the wall to act as a waveguide.

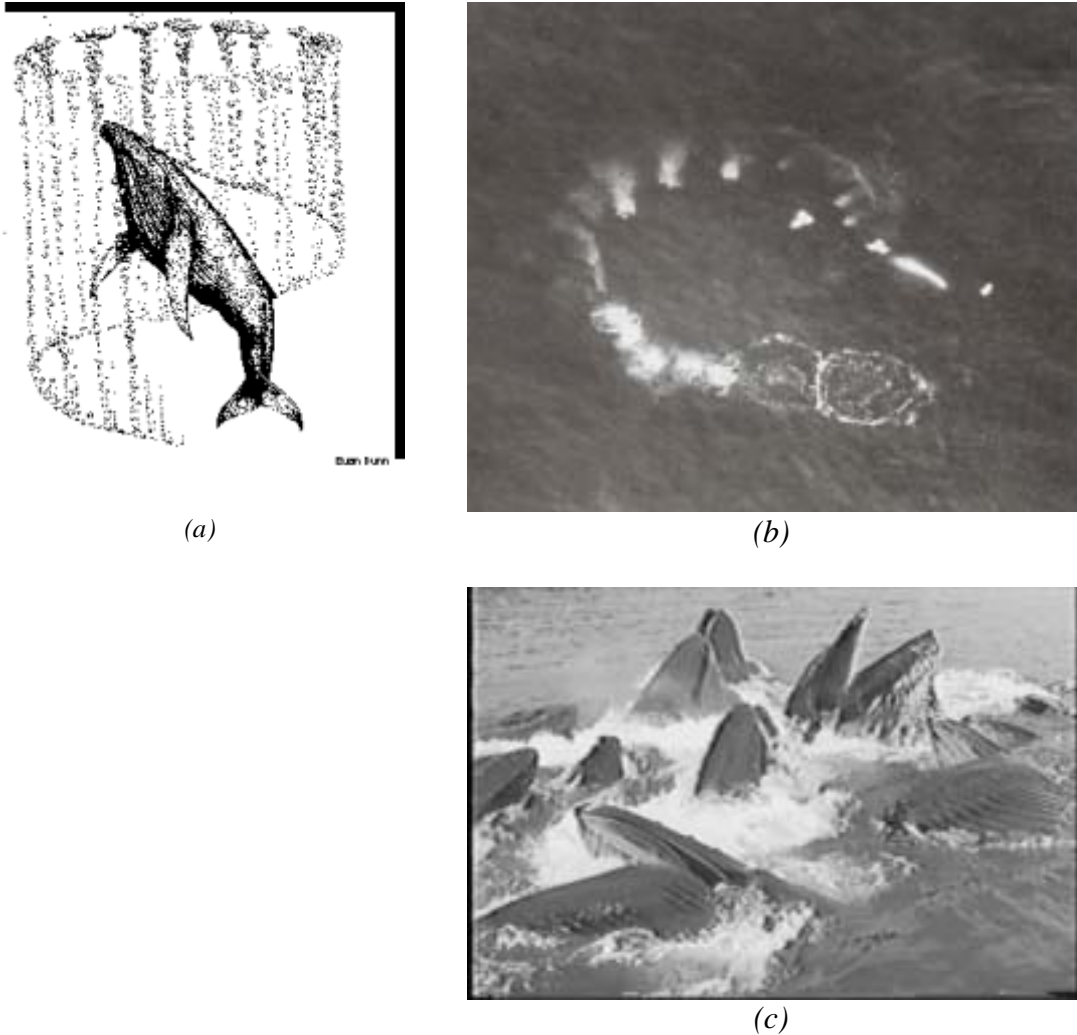


FIGURE 1. (a) Schematic of a humpback whale creating a bubble net. A whale dives beneath a shoal of prey and slowly begins to spiral upwards, blowing bubbles as it does so, creating a hollow-cored cylindrical bubble net. The prey tend to congregate in the center of the cylinder, which is relatively free of bubbles. Then the whale dives beneath the shoal, and swims up through the bubble-net with its mouth open to consume the prey ('lunge feeding'). Groups of whales may do this co-operatively (Image courtesy of Cetacea.org). (b) Aerial view of a humpback bubble net (photograph by A. Brayton, reproduced from [10]). (c) Humpback whales lunge feeding (Image courtesy of L. Walker, <http://www.groovedwhale.com>).

Assume the scales permit the use of ray representation. Figure 2 shows how, with tangential insonification,¹ the mammals could generate a 'wall of sound' around the net, and a quiet region within it. As fish approach the wall, swim bladder resonances may be excited. The natural schooling response of fish to startling by the intense sound as they approach the walls would, in the bubble net, be transformed from a survival response into one that aids the predator in feeding [8].

Figure 2*b* plots the raypaths (calculated using standard techniques [11]) from four whales for the stated launch conditions, for a bubble net in which the void fraction increases linearly from zero at the inner and outer walls, to 0.01% at the mid-line of the wall.

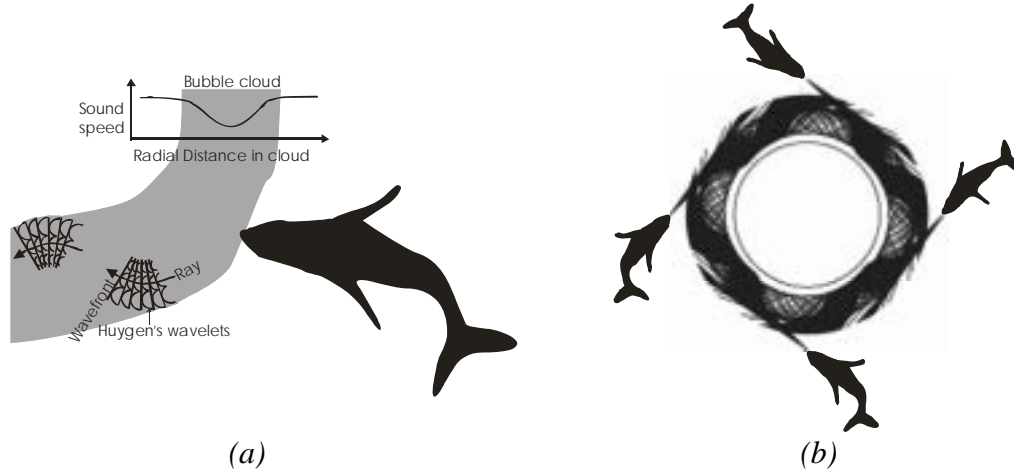


FIGURE 2. (a) Schematic of a whale insonifying a bubble-net (plan view), illustrating the sound speed profile in the cloud and, by Huygen's construction, sample ray paths. The sound speed profile assumes void fractions are greatest in the mid-line of the net wall, and assumes that the bubbles pulsate in stiffness mode. Hence the closer a Huygens wavelet is to the mid-line, the smaller the radius of the semicircle it forward-plots in a given time. Rays tend to refract towards the mid-line. (b) Four whales insonify an annular bubble net described in the text. The inner circle represents the inner boundary of the net wall. The outer boundary is obscured by the rays. Computed ray paths, where each whale launches 281 rays with an angular extent of 10° , refract as in (a). The rays gradually leak out, although some rays can propagate around the entire circumference. Plotting of a raypath is terminated when it is in isovelocity water and on a straight-line course which will not intersect the cloud. This refers to rays whose launch angles are such that they never intersect the net; and to rays which, having entered the net and undertaken two or more traverses of the mid-line, leave it. (Figure by T. G. Leighton, S. D. Richards and P. R. White [8]).

The actual acoustics of the cloud will, of course, be complicated by 3D effects and the possibility of collective oscillations; and even, speculatively, bubble-enhanced parametric sonar effects [12] which might be utilized by whales, for example to reduce beamwidth or generate harmonics, sum- and difference-frequencies etc.

The effect follows the frequency dependency described above. At frequencies sufficiently high to drive the bubble cloud in an inertia-controlled fashion, the bubbles produce in an increase in sound speed. The wall is outwardly-refracting, and rays are no longer trapped within the cloud. The refractive effect of these bubbles on sound speed becomes negligible at even higher frequencies, although of course acoustic attenuation and scatter may be great. A variety of ray behavior is possible, from reflecting straight off the net to traversing it and the interior with barely any refraction [8]. Such frequencies would not be effective in trapping prey, even if the prey could perceive them. However, if scattering losses permit (and it is by no means certain they would), is it possible that, given these refracted paths, such frequencies could be used for echolocation of the contents of the net?

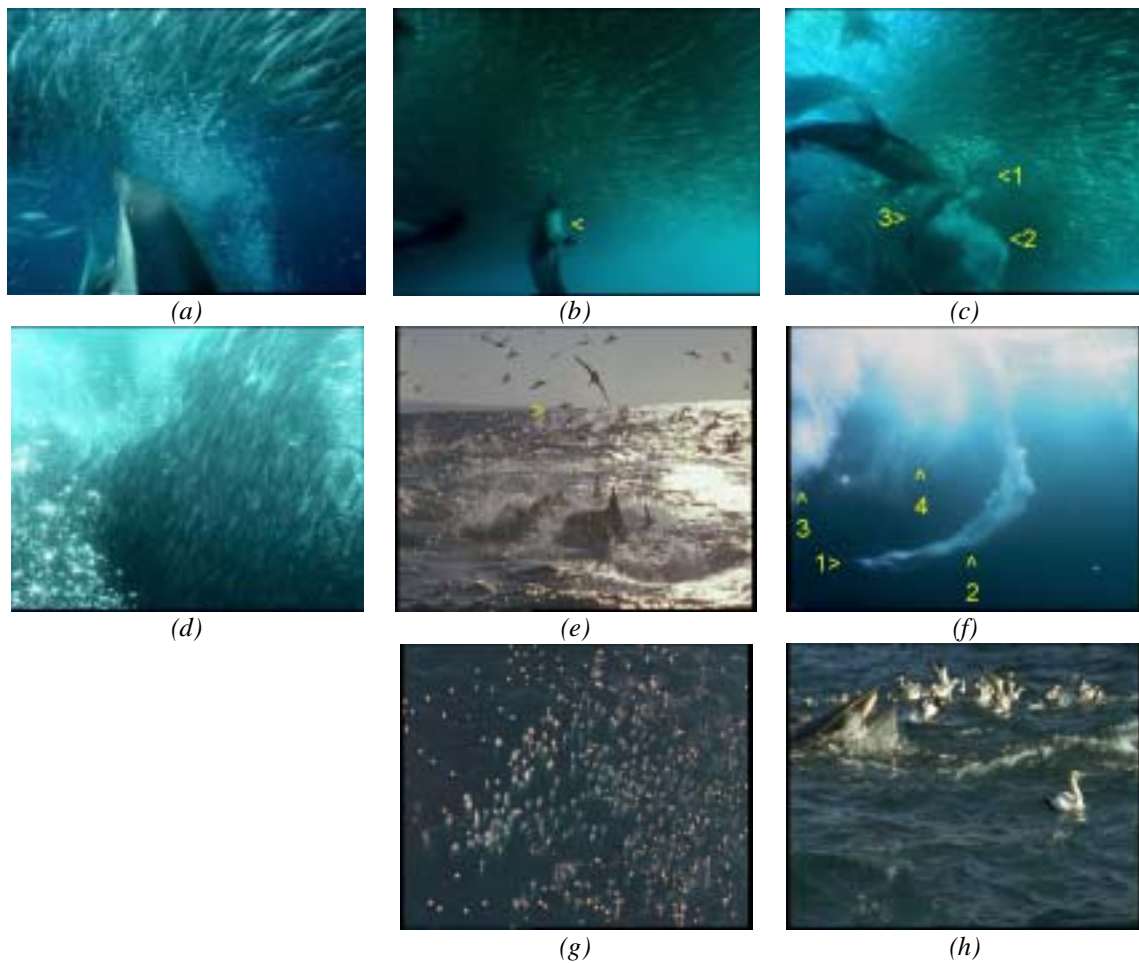


FIGURE 3. (a) Common dolphins herd sardines with bubble nets. (b) A dolphin starts to release a cloud of bubbles (arrowed) from its blowhole. A moment later (c) the dolphin (1) swims on, leaving behind the expanding cloud (2). Other dolphins (including the individual labeled '3') enter the frame. (d) The sardines school within a wall of bubbles that they are reluctant to cross, whilst (e) gannets dive into the sardine shoal to feed, folding their wings just before entry (arrowed). (f) On diving, a gannet (1) entrains a bubble plume (2). Plumes a few seconds old (3, with an older 4) have spread. (g) An aerial view shows hundreds of tight bubble plumes beneath airborne gannets. (h) A Bryde's Whale joins the feed. It surfaces with open mouth, which it then closes, sardines spilling from it. Images copyright of the The Blue Planet (BBC) and reproduced with permission. The accompanying book to the series is Byatt *et al.* [18].

With humpbacks the probability appears to be low. Echolocation is normally associated with *odontoceti*, and although there are suggestions that humpbacks may exploit it [13,14], there is to date no evidence that they have used it to locate schools of prey. Although there is evidence of directionality in the songs of humpbacks [15,16], Fig. 2*b* should not be interpreted as implying they can generate a 10° beam – we do not know one way or the otherⁱ. Similarly, the highest reported frequencies

ⁱ Even if the whales do not create beams that are sufficiently directional, and do not insonify tangentially, the bubble net might still function through its acoustical effects. The 'wall of sound' effect in Figure 2*b* is generated from those rays which impact the wall at low grazing angles. Those rays which never impact the wall do not contribute to the 'wall of sound'. If rays of higher grazing angle impact the net, they may cross into the net interior, though their amplitudes would be reduced by the bubble scattering, and attenuation alone would generate a quieter region in the center of the net.

generated by humpbacks correspond to harmonics in recordings in excess of 15 kHz [17] and 24 kHz [16], close to the bandwidth of the recording equipment. Exploitation of the inertia-controlled regime, as described above, would probably require higher frequencies. However, dolphins have also been observed to feed using bubble clouds [18] (Fig. 3*a-d*), and some can generate up to 170 kHz. It would be perhaps asking a lot for dolphins to identify fish among the strong bubble scatterers, although the environments which they naturally might encounter are similarly complex [19]. Either dolphins are accepting the loss of their echolocating abilities when they generate bubble nets to catch prey, or they have developed techniques for echolocating in bubbly water. Possible nonlinear ways to do this, which would suit the high amplitude signals and short ranges they would be working with, are discussed in relation to Fig. 5. The prospect of trapping low frequency sound in a bubble cloud to herd prey, while simultaneously echolocating with higher frequencies, is attractive but perhaps unlikely.

It may, however, be that exploitation of the schooling of fish in response to startling using bubble acoustics is more widespread, if perhaps less elegant, than the scheme of Figure 2*b*. The filming associated with Byatt *et al.* [18] shows bubble plumes generated by gannets (Fig. 3*e-g*) diving into a shoal of sardines which dolphins have herded to the sea surface. These plumes will no doubt complicate an underwater sound field already populated by the calls and bubble nets of dolphins, and the entrainment noise of the gannet bubble plumes, and could further stimulate the sardines to school [7]. Gannets, dolphins, sharks and whales etc. (Fig. 3*h*) all benefit from this, although to what extent this is intentional is unknown.

ATTENUATION AND SOUND SPEED IN NONLINEAR THEORY

Key to interpretation of (8) is the understanding that it is a generic framework. Depending on how $dV_j(t)/dP_i(t)$ is calculated for the bubbles within the population, it can be made applicable to linear or nonlinear bubble oscillation [2]; to bubbles in free field or reverberant conditions [20]; or to bubbles constrained by structures [21, 22], or surrounded by media other than pure water (such as tissue, sediment, or interacting bubbles) [23-26]. It is also through $dV_j(t)/dP_i(t)$ that a rigorous time-dependent attenuation can be calculated for bubbles undergoing nonlinear propagation [2].

Acoustic attenuation through bubble clouds has previously been predicted using the concept of acoustic cross-section. Predominantly this has been calculated for bubbles undergoing linear steady state pulsations [27]. However, in 1986 Akulichev *et al.* [28] produced a version which described the ring-up to steady state of the cross-section for semi-infinite monochromatic forcing, although this was strictly limited to resonant bubbles only. Two later studies [29, 30] attempted to extend Akulichev's formulation to off-resonant bubbles, but the method and results are unphysical. The cross-sections were constrained to ring up from an initial value (for which the quantitative basis was not strong) to the steady-state value, with the $(1 - e^{-\beta_{tot}t})H(t)$ time-dependency that Akulichev *et al.* had found for resonant bubbles. However, the pulsations of off-resonant bubbles do not display such a time-dependency [7]. A

physics-based time-dependent cross-section (for both single bubbles and clouds) was formulated by Clarke and Leighton [31], which properly accounted for the bubble time-dependency and initial conditions. However, while the model of bubble dynamics was nonlinear, the damping upon which the energy loss was calculated was based upon the losses associated with linear monochromatic bubble pulsations. Therefore, a fully nonlinear time-dependent cross-section, taking account of damping correctly, was later developed [2].

Much of this interest, in the time-dependency of scatter or attenuation from bubble clouds, historically arose to address a specific problem. This was, whether or not it could be exploited to extract the signal returned from a solid body (such as a mine) from that scattered by a bubble cloud whose own echoes are hiding the solid body. The ability to include nonlinearity in addition to time dependency, as this paper provides, greatly enhances this possibility. An example will be given in Fig. 5, after a demonstration of how nonlinearity can be included into the calculation of sound speed and attenuation.

As stated above, the method derives its description of the bubble environment (free field, in sediment etc.) from the model used to calculate $dV_j(t)/dP_i(t)$. For the calculations of this paper, the Keller-Miksis model was used [2], with thermal damping calculated after the manner of Prosperetti *et al.* [32, 33] and Nigmatulin *et al.* [34]. The results are explained in Figure 4, with comparison to the result if the linear steady-state formulation of Commander and Prosperetti [1] is used to calculate $dV_j(t)/dP_i(t)$.

Recall the earlier discussion of the plot of gas volume against applied pressure, applied to a single bubble subjected to a semi-infinite driving pulse. The locus consists of a single point until the onset of insonification. From this moment on, the locus describes orbits until reaching steady-state, after which it repeatedly maps out a given orbit. Assume the gas is perfect. Its internal energy U is a state function, such that whenever an orbit crosses its previous path, at both moments represented by the intersection the value of U is the same. More specifically, consider that:

$$dU = \bar{d}Q + \bar{d}W = \bar{d}Q - PdV \quad (9)$$

where the notation indicates that both the incremental heat supplied to the bubble ($\bar{d}Q$) and the work done on the bubble ($\bar{d}W$) are not exact differentials, whilst dU is.

Because Fig. 4 uses the applied acoustic pressure $P(t)$, the area mapped out by any loop represents the energy subtracted from the acoustic wave by the bubble in the time interval corresponding to the perimeter of the loop. This is because the bubble dynamics (such as the Keller-Miksis with thermal losses used here) may be interpreted simply as a statement of the equality between that pressure difference (Δp) which is uniform across the entire bubble wall, and a summation of other terms. These terms relate to the pressure within the gas and vapour inside the bubble (p_i), surface tension pressures (p_σ), and the dynamic terms resulting from the motion of the liquid required when the bubble wall is displaced [12], which will here be termed p_{dyn} :

$$\Delta p = p_i - p_{dyn} - p_\sigma \quad (10)$$

The energy subtracted from the sound field by the pulsating bubble in each circuit of a loop is given by:

$$E_{loop} = -\oint p_i dV + \oint p_{dyn} dV + \oint p_\sigma dV \quad (11)$$

(noting that the details of the chemistry on the bubble wall may make the final integral non-zero). However Δp equals the spatial average over the bubble wall of the blocked pressure $\langle p_{blocked} \rangle$, which in the long-wavelength limit equals the applied acoustic pressure $P(t)$ that would be present at the bubble centre were the bubble not present. Substituting (10) into (11) therefore shows that the area mapped in a loop in the pressure-volume plane is the energy subtracted from the acoustic wave in the time interval corresponding to that loop:

$$E_{loop} = -\oint \Delta p dV = -\oint \langle p_{blocked} \rangle dV \approx -\oint P dV \quad (kR \ll 1) \quad (12)$$

Therefore, the rate at which the acoustic field does work on the bubble can be found by integrating the area in the pressure-volume plane enclosed by the loops formed by the intersections described above, and dividing energy so obtained by the time interval taken to map out that loop. In this way the rate at which the bubble subtracts energy from the driving acoustic field can be calculated as a function of time, for example during bubble ring-up; and whilst steady state is strictly only achieved as $t \rightarrow \infty$, loops approximating to it can readily be identified (Fig. 4, middle row).

Of particular interest is the bottom row of Fig. 4, which superimposes the steady-state nonlinear loops of the middle row (thin line) with the corresponding linear solution using the formulation of Commander and Prosperetti (which is of course steady-state [1]; thick line). At frequencies much greater than or less than resonance (not shown), both models predict loci indistinguishable from straight lines (dissipation and nonlinearities being negligible at such extremes). The gradients of these lines have opposite signs, in keeping with the π phase change which takes place between the stiffness- and inertia-controlled regimes; and that sound speed is reduced in the first and increased in the second (through the sign of the gradient of dV_i/dP_i , after (7)). In such cases a sound speed can be readily calculated from (7) or (8). Closer to resonance, increasing dissipation imparts finite areas to the loops, and the sound speed must be inferred from the ‘spine’ of the loop.

While in some cases the nonlinear model would impart a similar spine to its loop as would that of Commander and Prosperetti (Fig. 4a, bottom row), closer to resonance identification of the optimum spine becomes more difficult (Fig. 4b, bottom row; note that the conditions for resonance in the nonlinear and linear models are slightly different). The increasing dissipation and ill-defined nature of the spine may lead to inaccuracies, and indeed Commander and Prosperetti note that ‘In the presence of resonance effects, the accuracy of the model is severely impaired’. This may not simply be due to the rapidity with which sound speed changes around a resonance, but also because errors associated with the free field assumption are greatest there [20].

In Fig. 4c, the nonlinear model displays a second harmonic (which is of course not apparent in the linear result). The ‘spine’ of this double-loop would be curved, and its

identification would allow calculation of nonlinear propagation through bubble clouds, waveform distortion, parametric signal generation etc.

With $dV_j(t)/dP_i(t)$ for the individual bubbles (and the cloud) varying through the oscillatory cycle, so too will the speed at which different regions of the acoustic wave will propagate. Hence, by combining nonlinear time-dependent data such as is presented in Fig. 4 for a single bubble, to generate the response of a given volume element of the bubble cloud, the sound speed for nonlinear propagation through the bubble cloud can be found in the usual manner [35].

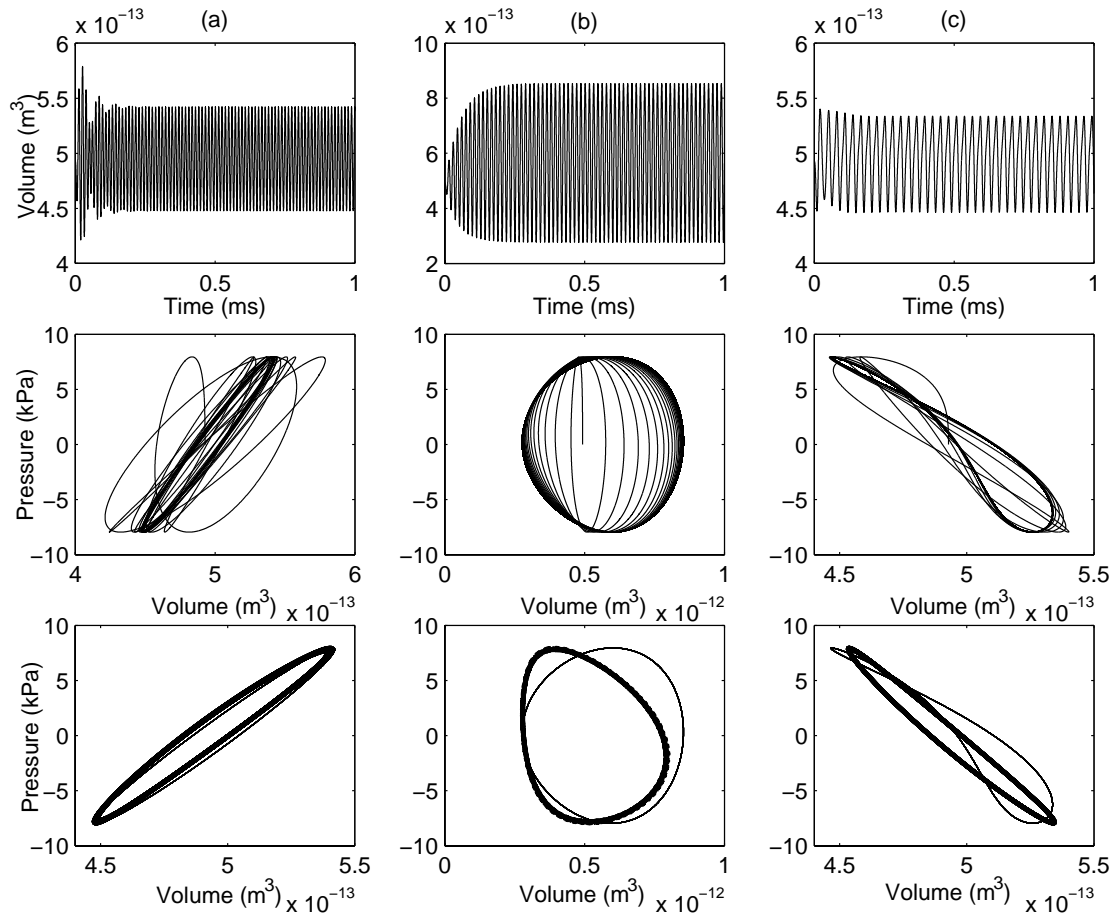


FIGURE 4. Bubble responses for a $49 \mu\text{m}$ bubble insonified by a semi-infinite pulse starting at $t=0$ with an amplitude of 7.95 kPa at (a) 84.2 kHz (b) 65.7 kHz and (c) 31.5 kHz . The top graph in each case shows the volume time history calculated using the Keller-Miksis equation (with damping after [32]). The middle graph in each case shows the corresponding pressure-volume curve. The darker area in each PV curve shows the steady state regime, where the successive loci overlap each other. Nonlinear components will cause crossovers in a loop (as in Fig. 4c where a second harmonic arises from driving the bubble close to half resonance frequency), such that the integration of (12) causes the areas of the clockwise loops to be subtracted from those of the anticlockwise. The bottom row superimposes the steady-state loops of the middle row (thin line) with the corresponding linear solution using the steady-state formulation of Commander and Prosperetti [1] (thick line). Figure by T. G. Leighton, S. D. Meers, and P. R. White [2].

APPLICATIONS FOR NONLINEAR PROPAGATION THROUGH BUBBLE CLOUDS

The above methodology has been used to:

- (1) Invert measured acoustic propagation characteristics in the surf zone to determine the bubble size distribution [2, 36], and compare the results with inversions undertaken using the linear technique of Commander and McDonald [37], which exploits the linear propagation of Commander and Prosperetti [1];
- (2) Predict the amplitude dependency of attenuation in oceanic bubble clouds [2];
- (3) Compare the errors which might accrue through neglect of the nonlinearity of bubble pulsations in high amplitude fields, with those which occur through neglect of bubble-bubble interaction [2];
- (4) Model the nonlinear response of biomedical contrast agents [38].

As stated at the outset, the ability to incorporate nonlinear bubble dynamics into models of acoustic propagation is not restricted to their use in systems where the void fraction is so high as to make high amplitude insonification an unavoidable necessity. With any bubble cloud, nonlinear pulsations can be generated and the results exploited as an additional diagnostic tool. Consider for example the problem scenario described earlier: Sonar fails to detect a linearly-scattering target (e.g. a solid body such as a mine, or a swim bladder insonified at frequencies much greater than its resonance), because the returned sonar signal is dominated by the scatter from bubble clouds in the vicinity of the target. If the scatter from the bubbles were linear, all that could be done to suppress their overwhelming contribution from the sonar return would be to try to exploit the time-dependence of the signal, as discussed earlier. However if the insonifying field were sufficiently high-amplitude to generate nonlinear response, it might be possible to enhance scatter from the target whilst simultaneously suppressing it from the bubbles. Consider if the insonifying field consisted of two high amplitude pulses, one having reverse polarity with respect to the other (Fig. 5, top line). Linear reflection from the target is shown in Fig. 5*b(i)*. The bubble generates nonlinear radial excursions (Fig. 5*a(i)*) and emits a corresponding pressure field (Fig. 5*a(ii)*). Normal sonar would not be able to detect the signal from the target (Fig. 5*b(i)*), as it is swamped by the return from the bubbles (Fig. 5*a(ii)*). If however the returned time histories are split in the middle and combined to make a time history half as long, enhancement and suppression occurs. If the two halves of the returned signals are added, the scattering from the bubble is enhanced (Figs. 5*a(iii)* and *a(iv)*), whilst the scatter from linear scatterers (such as the target) is suppressed (Fig. 5*b(ii)*). This can be used to enhance the scatter from biomedical contrast agents [7]. If however the two halves of each returned signal are subtracted from one another, the scattering from the bubbles is suppressed (Figs. 5*a(v)* and *a(vi)*) whilst the reflections from the linear target are enhanced (with the usual constraints imposed by increased signal-to-noise ratio) (Fig. 5*b(iii)*) [7].

CONCLUSIONS

This paper describes the method by which the sound speed and attenuation can be calculated for inhomogeneous bubble clouds subjected to pulses of arbitrary time history. The method provides a generic framework, such that the bubble cloud in question could be in a range of environments (such as in free field, in reverberation, in clouds of interacting bubbles, in sediments, in structures or *in vivo*) depending on the model used to calculate the dependence of the bubble volume on the insonifying field. Some applications are outlined.

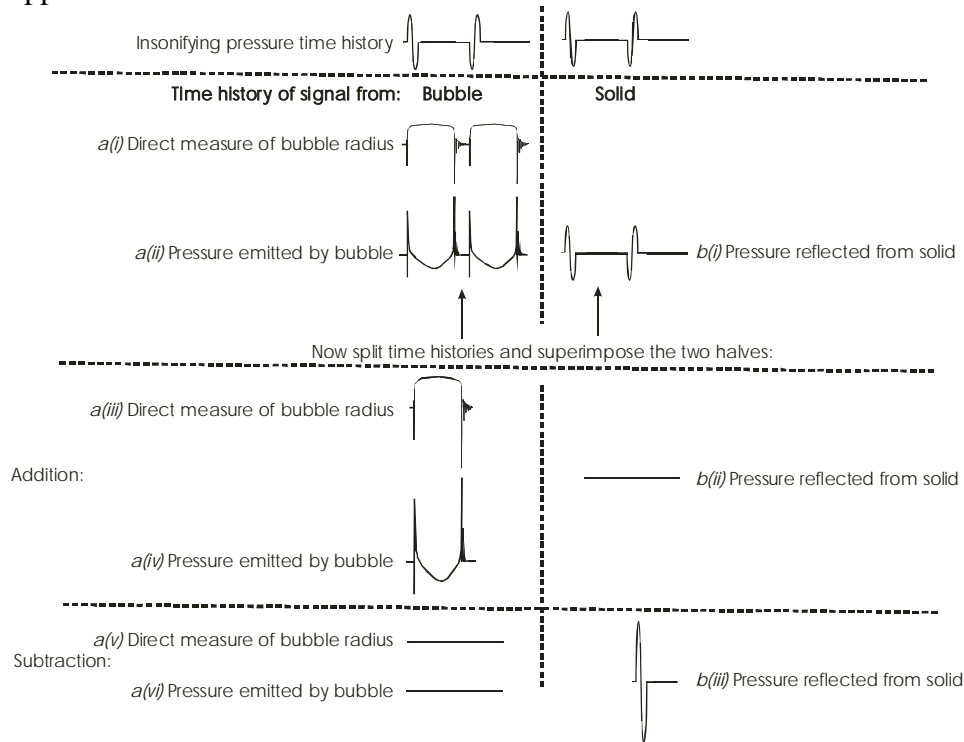


FIGURE 5. Schematic of a proposed ‘Twin Inverted Pulse Sonar’, whereby the scattering from a linear scatterer (such as a solid, a mine, or a swim bladder insonified at frequencies much greater than its resonance), and scattering from nonlinear scatterers (such as bubbles) can be enhanced and suppressed relative to one another (see text). The schematic bubble radius and time histories are justified in [7].

ACKNOWLEDGMENTS

The author would like to thank for the following for useful discussions: P. R. White, G. J. Heald, S. D. Richards, H. A. Dumbrell, C. L. Morfey. The author has made reasonable attempts to obtain permission to use the image in Figures 1*b*.

REFERENCES

1. Commander, K. W., and Prosperetti, A., *J. Acoust. Soc. Am.* **85**, 732-746 (1989).
2. Leighton, T. G., Meers, S. D., and White, P. R., Propagation through nonlinear time-dependent bubble clouds, and the estimation of bubble populations from measured acoustic characteristics, *Proceedings of the Royal Society* (in press; published Royal Society FirstCite website May), (2004).

-
3. van Wijngaarden, L., *J. Fluid Mech.* **33**, 465-474 (1968).
 4. Caflisch, R. E., Miksis, M. J., Papanicolaou, G. C., and Ting, L., *J. Fluid Mech.* **153**, 259-273 (1985).
 5. Farmer, D. M., and Vagle, S., *J. Acoust. Soc. Am.* **86**, 1897-1908 (1989).
 6. Buckingham, M. J., *Phil. Trans. R. Soc. Lond. A* **335**, 513-555 (1991).
 7. Leighton, T. G., From seas to surgeries, from babbling brooks to baby scans: The pressure fields produced by non-interacting spherical bubbles at low and medium amplitudes of pulsation, *International Journal of Modern Physics B* (in press) (2004).
 8. Leighton, T. G., Richards, S. D., and White, P. R., *Acoustics Bulletin* **29**, 24-29 (2004).
 9. Sharpe, F. A., and Dill, L. M., *Canadian Journal of Zoology-Revue Canadienne de Zoologie* **75**, 725-730 (1997).
 10. Williams, H., *Whale Nation*, London: Jonathan Cape (now part of Random House), 1988.
 11. Jensen, F. B., Kuperman, W. A., Porter, M. B. & Schmidt, H. *Computational Ocean Acoustics*. New York: Springer-Verlag, 2000.
 12. Leighton, T. G., *The Acoustic Bubble*, London: Academic Press, 1994, pp. 58-59, 288-301, 302-308.
 13. Frazer L. N., and Mercado, E., *IEEE J. Oceanic Engineering*, **25**(1), 160-182 (2000).
 14. Mercado, E. and Frazer L. N., *IEEE J. Oceanic Engineering*, **26**(3), 406-415 (2001).
 15. Levenson, C. "Characteristics of sound produced by humpback whales (*Megaptera novaeangliae*)," in *NAVOCEANO Technical Note 7700-6-72*. Washington, DC: Naval Oceanographic Office, 1972.
 16. Au, W. W. L., Pack, A. A., Lammers, M. O., Herman, L., Andrews, K., and Deakos, M., *J. Acoust. Soc. Am.*, **113**, 2277 (2003).
 17. Au, W., James, D., and Andrews, K., *J. Acoust. Soc. Am.*, **110**, 2770 (2001).
 18. Byatt, A., Fothergill, A., Holmes, M., and Attenborough, Sir David, *The Blue Planet*, BBC Consumer Publishing (2001).
 19. Leighton, T. G., and Heald, G. J., Chapter 21: Very high frequency coastal acoustics. In: *Acoustical Oceanography: Sound in the Sea*, edited by H. Medwin, Cambridge: Cambridge University Press, 2004 (in press).
 20. Leighton, T. G., White, P. R., Morfey, C. L., Clarke, J. W. L., Heald, G. J., Dumbrell, H. A., and Holland, K. R., *J. Acoust. Soc. Am.* **112**, 1366-1376 (2002).
 21. Leighton, T. G., White, P. R., and Marsden, M. A., *Acta Acustica* **3**, 517-529 (1995).
 22. Leighton, T. G., Cox, B. T., and Phelps, A. D., *J. Acoust. Soc. Am.* **107**, 130-142 (2000).
 23. Anderson, A. L., and Hampton, L. D., *J. Acoust. Soc. Am.*, **67**, 1865-1889 (1980).
 24. Anderson, A. L., Abegg, F., Hawkins, J. A., Duncan, M. E., and Lyons, A. P., *Continental Shelf Research*, **18**, 1807-1838 (1998).
 25. Kargl, S. G., Williams K. L., and Lim, R., *J. Acoust. Soc. Am.* **103**, 265-274 (1998).
 26. Kargl, S.G., *J. Acoust. Soc. Am.* **111**, 168-173 (2002).
 27. Medwin, H., and Clay, C. S., *Fundamentals of Acoustical Oceanography*, San Diego: Academic Press, 1998.
 28. Akulichev, V. A., Bulanov, V. A., and Klenin, S. A., *Sov. Phys. Acoust.* **32**, 177-180 (1986).
 29. Suiter, H. R., *J. Acoust. Soc. Am.* **91**, 1383-1387, (1992).
 30. Pace, N. G., Cowley, A., and Campbell, A. M., *J. Acoust. Soc. Am.* **102**, 1474-1479 (1997).
 31. Clarke, J. W. L., and Leighton, T. G., *J. Acoust. Soc. Am.* **107**, 1922-1929 (2000).
 32. Prosperetti, A., Crum, L. A., and Commander, K. W., *J. Acoust. Soc. Am.*, **83**, 502-514 (1988).
 33. Prosperetti, A., and Hao, Y., *Phil. Trans. R. Soc. Lond. A* **357**, 203-223 (1999).
 34. Nigmatulin, R. I., Khabeev, N. S., and Nagiev, F. B. *Int. J. Heat Mass Transfer*, **24**, 1033-1044 (1981).
 35. Morse, P. M., and Ingard, K. U., *Theoretical Acoustics*, Princeton: Princeton University Press, 1968 pp. 874-882.
 36. Leighton, T. G., *J. Acoust. Soc. Am.*, **110**, 2694 (2001).
 37. Commander, K. W., and McDonald, R. J., *J. Acoust. Soc. Am.* **89**, 592-597 (1991).
 38. Leighton, T. G., and Dumbrell, H. A., *Proceedings of the First Conference in Advanced Metrology for Ultrasound in Medicine (Journal of Physics Conference Series)* (2004, in press).